H storage efficiency and sorption kinetics in composite materials

R. Checchetto, N. Bazzanella, A. Miotello, P. Mengucci

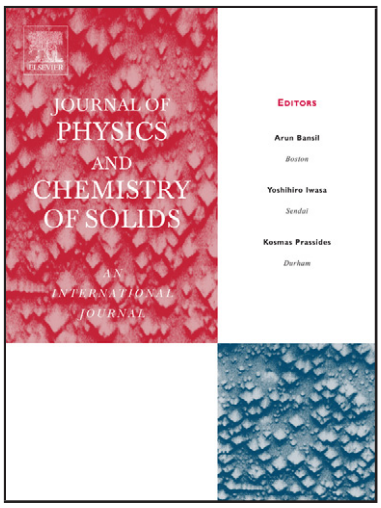

H_2 storage efficiency and sorption kinetics in composite materials

R. Checchetto, N. Bazzanella, A. Miotello, P. Mengucci

PII: S0022-3697(08)00094-2
DOI: doi:10.1016/j.jpcs.2008.03.032
Reference: PCS 5425

To appear in: *Journal of Physics and Chemistry of Solids*

Cite this article as: R. Checchetto, N. Bazzanella, A. Miotello and P. Mengucci, H_2 storage efficiency and sorption kinetics in composite materials, *Journal of Physics and Chemistry of Solids* (2008), doi:10.1016/j.jpcs.2008.03.032

H_2 storage efficiency and sorption kinetics in composite materials.

R. Checchetto[a], N. Bazzanella[a], A. Miotello[a] and P. Mengucci[b]

[a.] Dipartimento di Fisica dell'Università di Trento, I-38050 Povo (TN), Italy.

[b.] Dipartimento di Fisica ed Ingegneria dei Materiali e Territorio, Università Politecnica delle Marche, I-60131 Ancona, Italy

e-mail : checchet @science.unitn.it

Abstract

We have prepared two different kind of composite materials for hydrogen storage and studied their H_2 storage capacity and desorption kinetics. The first composite material consists of magnesium containing transition metal nanoclusters distributed in the Mg matrix (Mg:TM): this composite material shows better H_2 desorption performances than pure Mg. This improvement is attributed to the role of the MgH_2-TM nanocluster interface as preferential site for hexagonal Mg (h-Mg) nucleation and to the rapid formation of interconnected h-Mg domains where H diffusion during desorption occurs. The second composite material consists of $LaNi_5$ particles (size < 30 μm) distributed in a polymeric matrix. The H_2 storage capacity is negligible at low metal content (50 wt. %) when the metal particles are completely embedded in the polymeric matrix. The H_2 storage capacity is comparable to that of the pure $LaNi_5$ powders at high metal content (80 wt. %) when a percolative distribution is assumed by the $LaNi_5$ particles: this evidence points out the role of metal-metal interfaces and of interconnected metallic networks for H transport.

Keywords : Hydrogen Storage; Metal Hydrides; Polymers; Composite Materials.

1. Introduction.

Composite materials for hydrogen storage consist on a first (or more) component that absorbs large quantities of hydrogen and a second one (or more) that, in different ways, improves the operative performances of the system [1]. The first component is typically a hydride forming metal: these metals have high H_2 storage efficiency but present operative limitations that could impede their practical applications. Typical examples are: a) the pulverization of hydride particles upon repeated H_2 sorption cycles, as in the case of the low temperature forming hydride $LaNi_5$, b) the poisoning of the hydride surface after interaction with gases such as O_2 or H_2S as occurring with FeTi, c) the low thermal conductivity of the hydride phase, which is a problem common to most hydrides, and d) the slow H_2 sorption kinetics even after prolonged activation procedures at temperatures larger than 300°C, as occurring with pure Mg [2]. The second component of composite material improves the operative performances of the hydride forming metal by reducing the operative limits of one or more of the previously indicated processes.

In this communication we present a brief review on the H_2 sorption kinetics and storage capacity of two different composite materials that we have extensively studied in our research activity. The first one consists on a Mg matrix containing transition metal (TM) nanoclusters dispersed in the Mg bulk: here, the second component plays its role in the catalysis of the H_2 sorption kinetics by reducing the typical H_2 sorption times by up to two orders of magnitude [3-7]. The second composite sample consists on $LaNi_5$ particles, with size lower than 30 μm, dispersed in a polymeric matrix: here the polymer has a functional role as a binder that impedes the dispersion of the decrepitated fine $LaNi_5$ particles formed upon H_2 cycling [8]. The aim of this communication is to underline common features of these different composite systems by looking at the role of: a) the distribution of a component in the other one, 2) the interface between the two different materials, and c) the transport of the hydrogen species.

2. Experimental.

Composite samples consisting on Mg-TM samples (TM = Nb or Fe) were prepared in form of thick films (10 ÷ 20 μm) deposited on graphite wafers by r.f. magnetron sputtering. We used 99.97 % purity Ar as working gas and 99.95 % purity Mg as target material. The background pressure in the chamber was in the low 10^{-5} Pa order: the deposition process was carried out at 0.5 Pa Ar pressure and 150 W r.f. power without substrate heating. The metal doping of the Mg films was obtained by inserting small TM fragments over that part of the Mg target which is preferentially eroded by the Ar plasma and the metal content was controlled after deposition by Energy Dispersion Spectroscopy technique. The film samples deposited on polished graphite (g-C) peeled off from the substrates after exposure to air at ambient conditions. The activation procedure of the TM- doped Mg composite samples consisted on repeated absorption and desorption cycles at 623 K and 1.0 MPa H_2 [3,4]. While as prepared samples show an atomic distribution of the TM elements in the Mg layers, the activated samples, on the contrary, present a distribution of TM clusters with size in the 20 nm range, see the X-ray Diffraction (XRD) spectra presented in fig. 1 or refs. [4,5]. Here we present the H_2 sorption analysis carried out on samples with TM additive at content ~ 5 wt. % [4-7].

Polysiloxane is a class of polymeric materials available on the market which shows quite good characteristics of permeability to hydrogen gas in molecular form [9]: in the preparation of the second kind of composite material we used a self-curing acetic silicon formulation (*Saratoga*). $LaNi_5$ was selected since it is a standard hydride forming intermetallic compound with well-known performances. As-received polydispersed $LaNi_5$ product (SAES Getter) was fractioned by decantation in two fractions. The powder was dispersed into a high viscous polystyrene-chloroform solution and after a few minutes, the precipitate powder (containing the larger $LaNi_5$ particles) was separated from the supernatant, which contained the smaller $LaNi_5$ particles. Scanning Electron Microscopy (SEM) analysis indicates that the fraction containing the smaller particles was

composed by particles with size lower than 30 μm. This fraction was accurately washed by chloroform to completely remove all polystyrene traces from the metal surface and then used to prepare the composite samples. $LaNi_5$/polysiloxane composites were prepared by dispersing metallic powders to the liquid monomer under N_2 flux: the resin polymerization (cure) was carried out in air because oxygen is required for the reaction. Samples and metallic powders were stored under inert atmosphere (nitrogen) using a glove-box. Here we present the analysis carried out on composite specimens having size in the 1 mm order, with a metal content of ~ 50 (polymer-like sample, PL) and ~ 83 (metal-like sample, ML) wt. % [8]. In figs. 2(a) and 2(b) we present Environmental SEM micrographs of a section of the PL and ML, respectively, at 300 X magnification. We observe that while the PL sample shows well separated metallic domains, in the ML sample the $LaNi_5$ particles are in contact thus ensuring a high density of metal-metal interfaces. The activation procedure for the $LaNi_5$ powders and for the $LaNi_5$-polymer composite samples consisted on repeated H_2 absorption and desorption cycles at 353 K and 0.5 MPa.

3. Results and discussion.

In fig. 3 we present the H_2 desorption kinetics of pure MgH_2 and of Nb- and Fe- doped MgH_2 samples at the representative temperature of 623 K after loading at 1.2 MPa H_2 pressure: in the figure the reacted fraction α, that is the fraction of MgH_2 transformed in Mg, is plotted as function of time. We observe a strong improvement of the H_2 desorption kinetics given by the presence of the TM doping elements [3-7]. Curves show that both the h-Mg nucleation time, indicated in the figure by arrows, and the interval time required for the complete transformation of MgH_2 to h:Mg phase are much lower in the composite sample: 10 vs 10^3 s for h:Mg nucleation in the composite and pure MgH_2 sample, respectively, and ~ 10^2 vs ~ 10^3 for transformation after nucleation for composite and pure MgH_2 sample, respectively. These experimental results can be explained in the framework of the Johnson-Mehl-Avrami model. Analysis of the transformation curves evidence a transition from a prevailing continuous nucleation and growth process of the h-

Mg phase in the parent MgH_2 (pure MgH_2 sample) with 141 ± 5 kJ/mol activation energy, to a diffusion-controlled transformation in the doped MgH_2 sample characterized by 51 ± 5 kJ/mol activation energy [3-7]. We note that the activation energy pertinent to the diffusion-controlled transformation of the doped sample is very close to the value of the activation energy for H diffusion in the h-Mg phase [10]. Because the only difference between the activated pure and TM-doped MgH_2 samples is the presence of TM nanoclusters dispersed in the catalysed samples, we suggest that the pertinent transformation kinetics differ because:

a) the TM-MgH_2 interfaces act as preferential nucleation site for the h-Mg phase (this point explains why the interval time required for h-Mg nucleation process is negligible in the doped sample as compared to that in the pure one),

b) the average distance between the TM nanoclusters (~ 50 nm) is much shorter than the typical MgH_2 grain size (~ 1 μm). The transformed h-Mg domains, nucleated at the TM cluster surface, rapidly form an interconnected network where H dissociated from the residual MgH_2 phase preferentially migrates to the sample surface where its recombinative desorption occurs (this scheme both explains the prevailing diffusion character of the transformation and the evaluated activation energy).

A schematic diagram, representing the previously described nucleation and diffusion processes, is presented in fig. 4. Here, the black solid circles represent the TM nanoclusters embedded into the MgH_2 matrix which is represented as a gray background. The h-Mg phase is indicated by white squares, nucleated at the TM surface (fig. 4(b)) and forming interconnected domains ((fig. 4(c)).

In fig. 5 we present the Pressure-Composition (PC) isotherm (295 K) of the $LaNi_5$-polymer composite samples: the amounts of the absorbed H_2 are reported as weight % of the metal fraction only for the composite samples to allow a direct comparison with the performances of the $LaNi_5$ powders. In the figure, open circles and stars are pertinent , respectively, to the ML and PL samples while solid circles are experimental data pertinent to pure $LaNi_5$ powders [8]. The figure proves that hydrogen storage capacity close to that of the $LaNi_5$ powders can be obtained only in composite

samples with metal content close to 80 wt. %. The important morphological difference between the PL and ML samples is the presence of metal-metal interfaces in the ML sample while the PL samples only show metal-polymer interfaces. The lower hydrogen storage capacity of the PL sample can have different explanations:

i) Hydrogen dissolution into the metal requires molecular dissociation and H chemisorption via metal-hydrogen bond formation. When the metal domain is completely embedded in the polymer, it can be supposed that the metal surface is not active for molecular dissociation because the active sites for H_2 dissociation (in $LaNi_5$ they are generally Ni surface clusters) are bonded to the O atoms of the macromolecular back-bone by dative bond.

ii) Upon fractioning the $LaNi_5$ particles or during the composite sample preparation, the surface of the $LaNi_5$ particles can get poisoned. While the $LaNi_5$ powders or particles in the composite exposed to H_2 gas can be easily activated by repeated H_2 sorption cycles, this process cannot occur in the $LaNi_5$ particles completely embedded into the polymeric matrix as occurring in the PL sample.

iii) The exothermal nature of the metal to hydride phase transformation can offers the second explanation. The metallic particles are, in fact, embedded in the polymeric matrix and upon hydrogen absorption and the consequent metal to hydride phase transition they cannot dissipate efficiently the heat of transition thus increasing the temperature of the metallic particles.

We plan to clarify this point by analysing the H_2 storage performances of composite samples where the $LaNi_5$ particles are embedded in different polymers. We note anyway that the microstructure of the ML sample offers always a solution: interconnected metallic domains formed by metallic particles and metal-metal interfaces represent, in fact, diffusive paths where both the H diffusion process and heat transfer occur thus allowing a larger fraction of metallic particles to be hydrogenated.

In fig. 6 we present the H_2 desorption kinetics of the ML composite samples after loading at 295 K and 0.6 MPa H_2 pressure, (solid symbols) and, for comparison, that of the pure $LaNi_5$

powders [8]. Given a value of 10^{-8} cm^2/s order for the H diffusion constant both in the $LaNi_5$ hydride phase [11] and in the H-$LaNi_5$ interstitial solid solution [12], we can estimate a characteristic hydrogen diffusion time in the 10^3 to 10^4 s order over diffusion paths of ~1 mm, which is compatible with the characteristic H_2 desorption times of the ML samples. Just this point supports the idea of interconnected $LaNi_5$ metallic domains. H_2 storage in the PL sample is thus related to the hydrogenation of that small fraction of $LaNi_5$ particles, probably those at the composite sample surface.

We conclude this communication by remarking two points. The role of interfaces and migration paths for hydrogen, evidenced in the present composite samples, is similar to that suggested in ball-milled materials where the milling process induces the formation of a nanocrystalline structure. The high density of grain boundaries enhances the H_2 sorption kinetics because: i) the hydrogen transport is accelerated along these extended defects as compared to that in the crystal, and ii) the nucleation of new phases is here energetically favoured [13]. We also remark that some recent publications indicate that in ball-milled materials transition-metal (Nb) or transition-metal-oxide nanoparticles (Nb_2O_3) play a more complex role than that of surface catalysis for H_2 dissociation and recombination. The milling process gives rise, in fact, to a composite sample consisting on Nb or Nb_2O_3 nanoclusters embedded in the MgH_2 matrix: in the hydrogen desorption process the catalyst nanoclusters react with the liberated Mg forming ternary Nb-Mg-O domains that, distributed in the MgH_2 sample, form a network of pathways that facilitate the hydrogen transport [14,15].

4. Conclusions.

In composite samples for hydrogen storage where one of the phase consists on a hydride forming metal and the other on TM component, the H_2 storage capacity and sorption kinetics are related to the presence of extended internal interfaces and on the formation of a metallic network where H transport occurs. In MgH_2-TM composite the hydride-TM interface act as preferential site for h-Mg nucleation and the rapid formation of interconnected h-Mg domains produces the metallic network for H diffusion. In $LaNi_5$-PS composite the metal-polymer interface is not active for H_2 dissociation and an efficient H_2 storage occurs only at high metallic content when metal-metal interfaces allow the formation of interconnected $LaNi_5$ domains.

Acknowledgements

The research activity is financially supported by the Hydrogen-FISR Italian project.

References.

[1] A. Zaluska, L. Zaluski and J. O. Stroem-Olsen, Appl. Phys. **A72**, 157 (2001).

[2] G. Sandrock, J. Alloys Comp. **293-295,** 877 (1999).

[3] N. Bazzanella, R. Checchetto and A. Miotello, Appl. Phys. Lett. **85**, 5212 (2004).

[4] R. Checchetto, N. Bazzanella, A. Miotello and P. Mengucci, J. Alloys Comp. **404-406**, 461 (2005).

[5] R. Checchetto, N. Bazzanella, A. Miotello, C. Maurizio, F. D'Acapito, P. Mengucci, G. Barucca and G. Majini, Appl. Phys. Lett. **87**, 061904 (2005).

[6] N. Bazzanella, R. Checchetto, A. Miotello, C. Sada, P. Mazzoldi and P. Mengucci, Appl. Phys. Lett. **89**, 014101 (2006).

[7] R. Checchetto, N. Bazzanella, A. Miotello and P. Mengucci, J. Alloys Compd. (2006), doi:10.1016/j.jallcom.2006.11.017

[8] R. Checchetto, G. Carotenuto, N. Bazzanella and A. Miotello, J. Phys. D: Appl. Phys. 40, 4043 (2007).

[9] T. C. Merkel, V. I. Bondar, K. Nagai, B. D. Freeman and I. Pinnau, Journal of Polymer Science, Part B: Polymer Physics **38,** 415 (2000).

[10] J. Renner and H. J. Grabke, Z. Metallkd. **67**, 639 (1978).

[11] R. F. Karlicek and I. J. Lowe, J. Less-Common Met. **73,** 219 (1980).

[12] H. Zuechner, T. Rauf and R. Hempelmann , J. Less-Common Met. **172-174,** 611 (1991).

[13] J. Huot, G. Liang and R. Schulz, Appl. Phys. **A72**, 187 (2001).

[14] H. Gijs Schimmel, J. Huot, L. C. Chapon, F. D. Tichelaar and F. M. Mulder, J. Am. Chem. Soc. **127**, 14348 (2005).

[15] O. Friederichs, J. C. Sanchez-Lopez, C. Lopez-Cartes, T.Klassen, R. Bormann and A. Fernandez, J. Phys. Chem. **B110**, 7845 (2006)

Figure captions.

Fig. 1 : XRD spectra of activated MgH_2-TM composite samples.

Fig. 2 : Environmental SEM micrographs of a section of the ML (a) and PL (b) composite samples at 300 X magnification.

Fig. 3 : H_2 desorption kinetics of pure MgH_2 and of Nb- and Fe- doped MgH_2 samples at the representative temperature of 623 K.

Fig. 4 : Schematic diagram representing the H_2 desorption process from the TM doped MgH_2 composite sample as described in the text. The figure presents: (a) the initial situation, (b) the formation of the h-Mg domains at the MgH_2-TM interface, and (c) the formation of a network of interconnected h-Mg transformed domains. The black solid circles represent the TM nanoclusters embedded into the MgH_2 matrix described as a gray background while the h-Mg phase is indicated by white squares.

Fig. 5 : Pressure-Composition (PC) isotherm of the $LaNi_5$-polymer composite samples at 295 K. Open circles : ML composite. Stars : PL composite. Solid circles : pure $LaNi_5$ powders.

Fig. 6 : H_2 desorption kinetics of the ML composite samples after loading at 295 K and 0.6 MPa H_2 pressure and pure $LaNi_5$ powders.

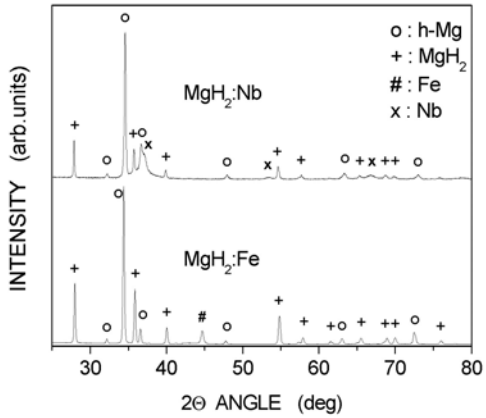

FIG. 1

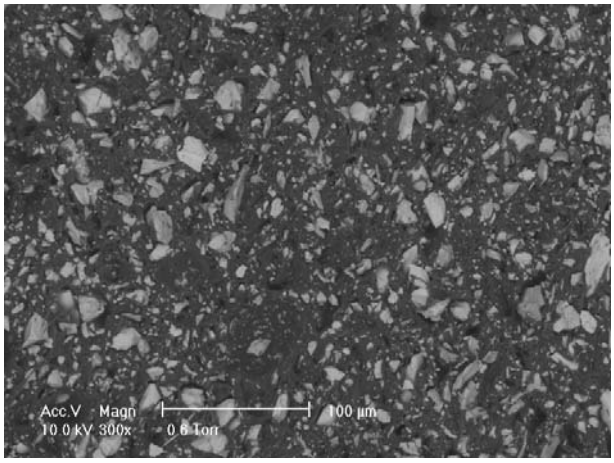

FIG. 2(a)

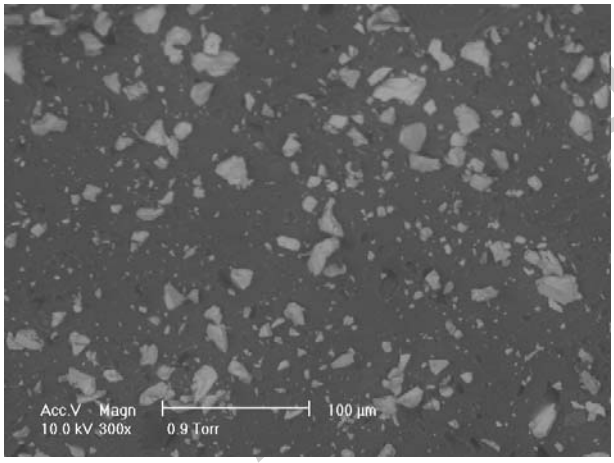

FIG. 2(b)

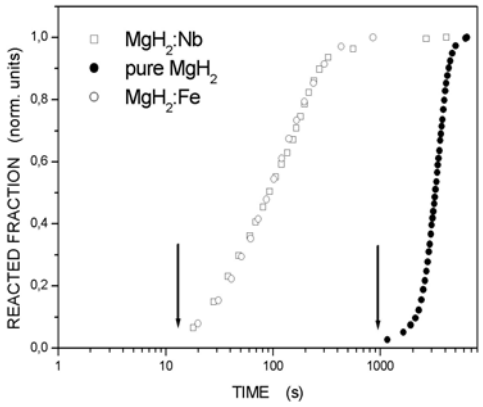

FIG. 3

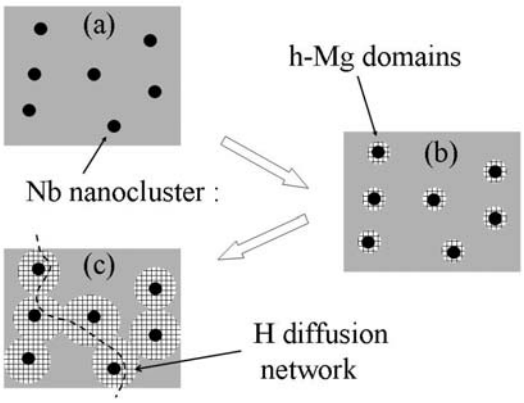

FIG. 4

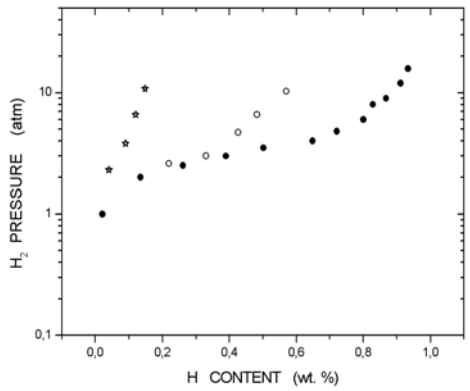

FIG. 5

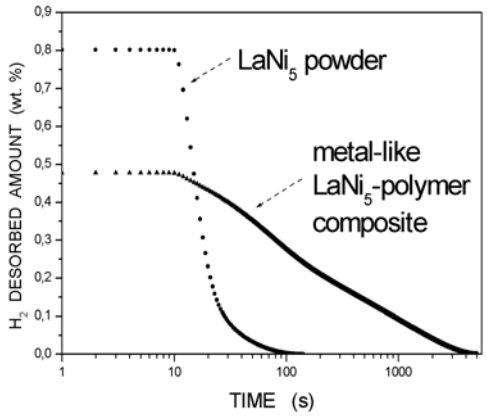

FIG. 6